29th International Cosmic Ray Conference Pune (2005) **5**, 13–16

A source stacking analysis of AGN as neutrino point source candidates with AMANDA

A. Gross[a] and T. Messarius[a] for the IceCube Collaboration
(a) Institute for Physics, University of Dortmund, D-44221 Dortmund, Germany
Presenter: T. Messarius (gross@physik.uni-dortmund.de), ger-gross-A-abs1-og25-poster

Source stacking methods have been applied in γ-astronomy and in optical astronomy to detect generic point sources at the sensitivity limit of the telescopes. In such an analysis, the cumulative signal and background of several selected sources of the same class is evaluated. In this report we introduce a systematic classification of AGN into several categories that are each considered as a TeV neutrino source candidate. Within each of these AGN categories the individual sources are stacked and tested for a cumulative signal using the AMANDA-II data.

1. Introduction

Active Galactic Nuclei (AGN) are known high luminosity photon emitters reaching photon energies up to some ten TeV. Additionally they are candidates for the production of high energy charged particles and neutrinos. A detection of TeV neutrinos (ν's) from AGN would provide invaluable insight into their nature and their contribution to the measured flux of high energy charged particles in cosmic rays.

AMANDA-II is a neutrino telescope operating at the geographic South Pole [1]. In AMANDA-II point source analyses [2, 3, 4], no statistically significant signal from any point source has been detected yet. The most sensitive analysis is based on data collected in 2000-2003 [4]. A further increase in sensitivity may be achieved by evaluating the same data set for the cumulative signal of several AGN. A source stacking analysis has been developed using individual classes of AGN that have been systematically categorized [5].

For each AGN type, the number of sources is optimized for the analysis with AMANDA-II. The samples are analyzed for a cumulative neutrino flux using the data set of the point source analysis [4].

2. AGN classification and selection scheme

With the aid of a systematic classification of AGN, we define categories of AGN for which individual AGN in each category are stacked. A large diversity of AGN types (like Seyfert galaxies, radio galaxies or quasars) has been observed and has historically been classified and named due to their appearance in telescopes sensitive to various wavelengths at Earth. The differences between the various AGN types may partially be explained by a unified geometrically axisymmetric model [6].

In Fig. 1, we present an AGN classification scheme depending on host galaxy, luminosity and angle of observation. A schematic view of an AGN is shown in Fig. 2. AGN are generally divided into radio-loud and radio-weak sources as it is indicated in the first branching of the classification scheme. Radio-loud AGN are mostly found in elliptical galaxies, while radio-weak ones are mostly located in spiral galaxies [7]. Radio-loud AGN with large scale jets show different morphologies depending on the luminosity at 178 MHz [8].

The catalogs which are used for the selection of generic source classes are listed at the bottom of Fig. 1 (black squares). A list of compact radio-loud objects, possibly young AGN where the jets are stopped in dense matter, is given by a sample defined in [9]. Blazars are radio-loud AGN observed in jet direction, including subclasses

of different luminosity at low radio frequencies, Flat Spectrum Radio Quasars (FSRQ) and BL Lac objects. Blazar emission is dominated by relativistic beaming effects and characterized by a flat radio spectrum. Radio galaxies, which are radio-loud AGN observed at a high inclination angle, are selected by their radio flux at 178 MHz as provided by the 3CR catalog. The radio galaxies are further divided into FR-I and FR-II radio galaxies, depending on different jet morphologies which are correlated with the luminosity at 178 MHz [8]. A sample of radio-weak quasars is defined by the Bright Quasar Survey, selected at optical and ultraviolet frequencies.

Further details of the classification can be found in [5].

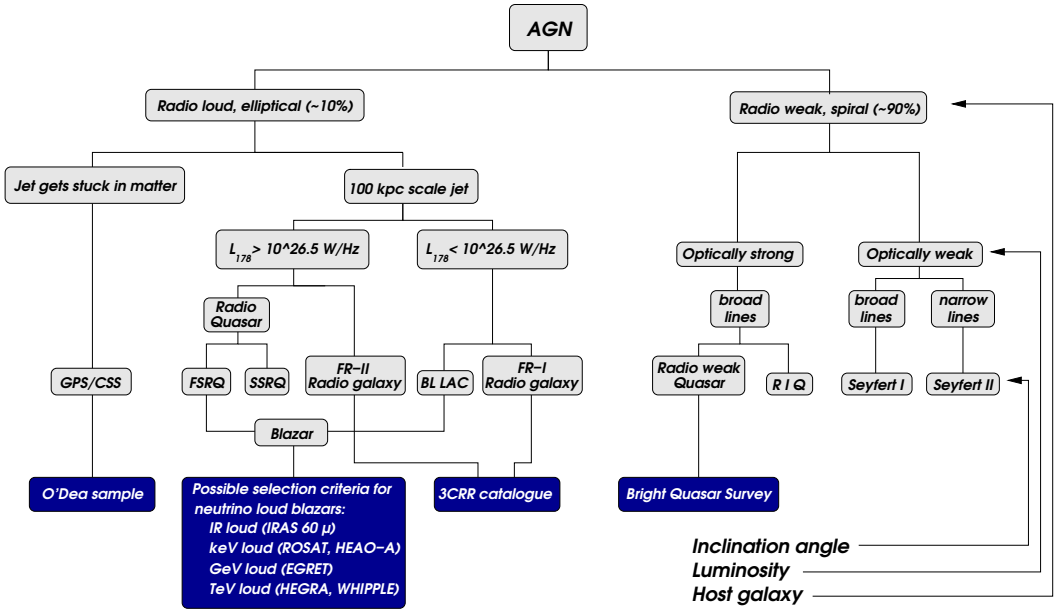

Figure 1. AGN classification according to host galaxy, luminosity and inclination angle. In the scheme, SSRQ and FSRQ stand for steep spectrum radio quasar resp. flat spectrum radio quasar. Radio intermediate quasars are labeled RIQ. The GHz Peaked Sources and the Compact Steep Spectrum sources are represented by GPS/CSS.

In most theoretical models for ν production in AGN, the dominant ν production mechanism is the decay of charged pions. The pions are decay products of the Δ resonance produced by pp or $p\gamma$ interactions of high energy protons. In AGN, the jets and the accretion disk are possible acceleration sites for protons.

In this scenario, the production of ν's is always coincident with the production of a similar number of γ's from the decay of neutral pions. For an observer at the Earth, the different optical depths for the propagation of neutrinos and photons may affect the spectra. The high cross sections of photons, e.g. for pair creation, mean a higher probability that photons will interact or be absorbed in the source region or in the interstellar medium. Then, the energy of the photons gets redistributed on several photons of lower energy and the γ flux is shifted to lower energies than the ν flux.

The ν production scenario motivates a selection of candidate sources from the various AGN classes according to their photon flux. The possible cascading of photons suggests considering also photon energies which are lower than the energy threshold of AMANDA-II for neutrinos, which is at about 50 GeV. For blazars, different selections are made according to their measured flux at IR, keV, GeV and TeV energies. Radio-weak quasars are selected according to their photon flux at 60 μm. For FR-I and FR-II radio galaxies, the radio flux at 178

MHz is used as the selection criterion. The compact objects (GPS and CSS) are sorted according to their optical strength.

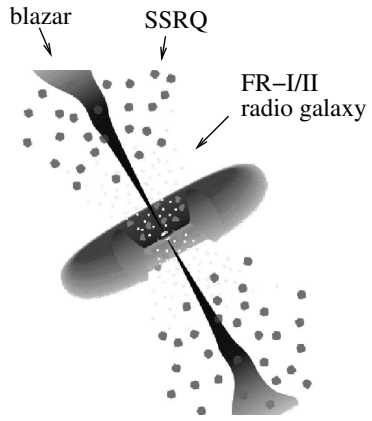

Figure 2. Scheme of an AGN with a black hole in the center and an accretion disc perpendicular to the direction of two jets along its rotation axis.

The number of sources in each generic sample is determined by the assumption, that the hypothetical ν flux at TeV energies is proportional to the photon flux at the selection energy. The normalization of the hypothetical signal is chosen in a way that the signal of the strongest source of each sample does not exceed the sensitivity of the point source analysis.

For most AGN categories, we found the optimum number of sources to include for the AMANDA-II analysis was about ten. The exceptions are FR-I and FR-II radio galaxies where specific distributions of the candidate sources constraint source stacking. FR-I galaxies are strongly dominated by the local source M87, while many FR-II galaxies show a comparable γ flux. Thus, for FR-I galaxies, the analysis of only M87 turns out to be most sensitive. In contrast, there is no optimum number of FR-II galaxies above which the expected sensitivity is decreasing. In this case the techniques of point source analysis become less suitable to analyze the signal than the search for an isotropic flux.

Even though in these two cases source stacking seems to be less sensitive to the hypotheses than other analyses, we look also at samples of these sources. For FR-II galaxies, this takes into account that point source methods are complementary to diffuse methods. For FR-I galaxies the possibility that M87 may be an exception from a general correlation motivates the consideration of an additional sample of FR-I galaxies where M87 is excluded. For a source listing of all samples see [5].

3. Data analysis

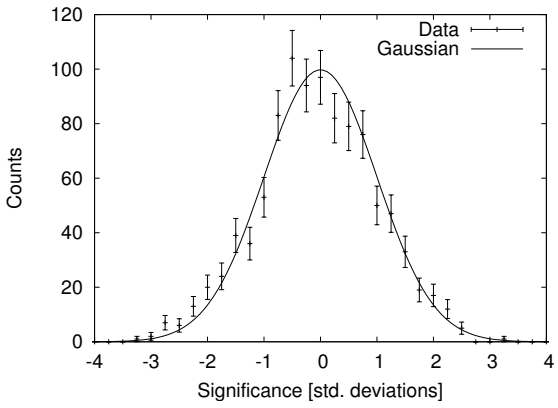

Figure 3. Significance distribution for hypothetical source samples with random positions.

For the samples of the AGN categories as selected above, the cumulative signal was evaluated with a data sample of events collected with AMANDA-II in the year 2000 [10]. None of the AGN categories had a statistically significant deviation from the background expectation [11, 5]. Here, we present an application of the method to a data set collected with AMANDA-II in 2000-2003 [4]. All optimization steps for the stacking results were redone, resulting in no significant change in the number of sources to include. The optimum bin size was found at a radii of $2.3 - 2.5°$, which is about 15% smaller than for the previous sample.

For the evaluation of a possible signal, the number of background events expected in a circular search bin around each source is assumed to be proportional to the event density in the zenith band of that source. Events which are in overlapping bins contribute only once to the cumulative signal. The back-

ground expectation for the stacked sources is corrected for the background expectation of the overlap regions. In this way, a double count of statistical fluctuations in overlapping bins is avoided. The analysis was tested in various ways. In total, 1000 test data sets with randomized right ascension (RA) for all events were generated. The resulting distribution of on-source counts is in agreement with the expectation from Poisson statistics. Additionally, a collection of samples containing 10 hypothetical sources with random source positions was analyzed, using the final data set (without randomization of RA). Also in this case, no deviations from the expectations were found. The significance distribution for these test data sets is shown in Fig. 3.

AGN category	N_{src}	N_ν^{obs}	N_ν^{bg}	f_{sens}
GeV blazars	8	12	20.5	1.5
unid. GeV sources	22	62	60.1	2.6
IR blazars	11	30	34.1	2.0
keV blazars (HEAO-A)	3	7	11.0	1.4
keV blazars (ROSAT)	8	19	25.8	1.8
TEV blazars	5	14	18.3	1.5
GPS and CSS	8	16	22.7	1.7
FR-I galaxies	1	2	2.5	0.7
FR-I without M87	17	28	45.0	2.4
FR-II galaxies	17	58	53.8	2.6
radio-weak quasars	11	29	32.5	2.1

Table 1. Results of the stacking analysis for each AGN category: the number of included sources is given by n_{src}, the number of expected events is listed under n_{bg} and the number of observed events is given by n_ν. The sensitivity of the analysis is listed under f_{sens} in units of $10^{-8}\mathrm{cm}^{-2}\mathrm{s}^{-1}$ for the integral flux above 10 GeV.

The evaluation of the signal yields no excess for any of the considered AGN categories. The observed and expected event counts for the selected AGN samples are listed in Table 1 together with the sensitivity to a flux from the corresponding AGN category. The sensitivities are given at 90% C.L. and do not include systematic errors. Limits on the flux from the considered AGN categories will be given after the investigation of systematic errors.

With help of the stacking analysis, the sensitivity per generic source has been lowered by a factor of 3 for a typical AGN category. No evidence of a signal has been found.

References

[1] http://amanda.uci.edu
[2] J. Ahrens et al., Phys. Rev. Lett. 92, 070201 (2004).
[3] M. Ackermann et al., Phys.Rev. D71, 077102 (2005).
[4] M. Ackermann, E. Bernardini, T. Hauschildt et al., these proceedings.
[5] M. Ackermann et al., to be published.
[6] C. M. Urry, P. Padovani, PASP 107, 803-845 (1995).
[7] M. O'Dowd, C. M. Urry and R. Scarpa, Astrophys.J. 580, 96-103 (2002).
[8] B. L. Fanaroff, J. M. Riley, Mon. Not. R. Astr. Soc. 167, 31-36 (1974).
[9] C. P. O'Dea, PASP 110, 493-532 (1998).
[10] J. Ahrens et al., Phys. Rev. Lett. 92, 070201 (2004).
[11] A. Groß et al., in: Proceedings of 40th Rencontres de Moriond on Electroweak Interactions and Unified Theories
[12] http://icecube.wisc.edu